Received 15 May 2019; revised 23 July 2019; accepted 23 August 2019. Date of publication 27 August 2019; date of current version 30 September 2019.
The review of this article was arranged by Editor K. Shenai.

Digital Object Identifier 10.1109/JEDS.2019.2937837

Experimental Investigations Into Temperature and Current Dependent On-State Resistance Behaviors of 1.2 kV SiC MOSFETs

KANG HONG, XIAO-YUAN CHEN (Member, IEEE), YU CHEN (Student Member, IEEE), MING-SHUN ZHANG, JIA-LEI WANG, SHAN JIANG, ZHOU PANG, HAN-MEI YANG, NING XUE, HUA-YU GOU, AND LEI ZENG

School of Engineering, Sichuan Normal University, Chengdu 610101, China

CORRESPONDING AUTHOR: X.-Y. CHEN (e-mail: chenxy44@sina.com)

This work was supported in part by the National Natural Science Foundation of China under Grant 51807128, and in part by the National Training Program of Innovation and Entrepreneurship for Undergraduates under Grant 201910636099, Grant 201910636017, Grant 201910636087, and Grant 201910636107.

ABSTRACT Performance characterization for long-time operation of cryogenic SiC MOSFETs remains as a challenge that requires further investigation. This paper presents experimental investigations into temperature and current dependent on-state resistance behaviors of state-of-the-art 1.2 kV SiC MOSFETs from various well-known semiconductor manufacturers. In view of engineering applications, two fitted double-exponential functions are introduced to visually depict the interactions among the on-state resistance, junction temperature and drain current instead of considering the combined effects of electron mobility and ionized dopant concentration inside cryogenic SiC MOSFETs. Optimal operating temperature and current ranges are subsequently extracted to characterize the cryogenic operation performance, and thus to explore some operating and designing guidelines of cryogenic SiC MOSFETs and SiC-based power conversions at 77 K.

INDEX TERMS Silicon carbide, SiC MOSFET, on-state resistance, liquid nitrogen, cryogenic power conversion.

I. INTRODUCTION

Silicon carbide (SiC) MOSFETs have been attracting tremendous attention for high-power applications, owing to their wide-temperature reliabilities offered by SiC over Si. To clarify and optimize the performance of SiC MOSFETs at different operating temperatures, a number of theoretical and experimental studies have reported the characterization of temperature dependences of various crucial parameters such as breakdown voltage, threshold voltage, and on-state resistance. Similar to abrupt P-N junctions, breakdown voltage of SiC MOSFETs also decreases with the temperature. Intuitively, this is due to the mean free path of charge carriers becomes larger and then offers more energy before collisions at a lower temperature [1]. On the contrary, threshold voltage increases with the decrease of temperature because a larger amount of electrons is trapped in the interface states and a higher voltage is then required to form the inversion channel at a lower temperature [2], [3].

Drain-source on-state resistance $R_{\mathrm{DS(on)}}$, which is normally used to quantify the conduction loss and energy efficiency, consists mainly of channel resistance, bulk resistance, drain and source contact resistances, substrate resistance, JFET resistance, etc [4], [5]. Due to the competing temperature dependences of the channel resistance and bulk resistance inside the SiC MOSFET device [6], [7], the total drain-source on-state resistance increases first and then decreases along with the decrease of operating junction temperature. The current literatures focus mainly on the performance of SiC MOSFETs at high temperatures up to 200°C or above [8]–[10], though very little has been reported with regard to the cryogenic operations of SiC MOSFETs at negative temperatures [11], [12]. Moreover, even in the most of cryogenic performance investigations of SiC MOSFETs at present, some pulsed currents having their lasting durations of tens to hundreds of microseconds are normally applied to test and evaluate the temperature-dependent and

This work is licensed under a Creative Commons Attribution 4.0 License. For more information, see http://creativecommons.org/licenses/by/4.0/

current-dependent $R_{DS(on)}$ behaviors. The results obtained in pulse current tests can be regarded as "instantaneous values" at some pre-set environment temperatures and drain currents. However, these characterizations are still insufficient for continuous operations of SiC MOSFETs [1]–[12] because practical junction temperature inside one SiC MOSFET is always higher than the environment temperature by considering the self-heating effect [13], [14]. Actually, dynamic thermal imbalance between the power dissipation inside one SiC MOSFET and the cooling power from external refrigerating fluid might aggravate the temperature rise along with the operating time, and even result in overheating damage in the case of overcurrent operations.

As a promising power conversion technology, SiC MOSFET based cryogenic power conversion suits to combine with zero-resistance superconducting inductor devices having self-contained cryogenic liquid nitrogen (LN_2) environment at 77 K, and replacing copper inductors and room-temperature SiC MOSFETs by superconducting inductors and cryogenic SiC MOSFETs can be well expected to improve the overall energy efficiency and eliminate the overheating risks of power electronics [15]–[17]. In our previous works in [15], we have investigated into the cryogenic operating behaviors of 650 V Si MOSFETs towards a Si-based cryogenic power conversion technology. As a subsequent study, this work attempts to present experimental investigations into temperature and current dependent $R_{DS(on)}$ behaviors of 1.2 kV class SiC MOSFETs, with aims to characterize the long-time cryogenic performance and thus to explore some operating and designing guidelines for SiC-based cryogenic power conversions.

II. EXPERIMENTAL DETAILS

In the experiments, five types of 1.2 kV class SiC power MOSFETs from various semiconductor manufacturers are tested and numbered as follows: 1) Type A - C2M0080120D from CREE; 2) Type B - SCT20N120 from STMicro- electronics; 3) Type C - SCT3080KL from ROHM Semiconductor; 4) Type D - UJC1206K from UnitedSiC; 5) Type E - LSIC1MO120E0080 from Littelfuse.

To obtain a continuous temperature-changing environment, the back conductive plate of drain electrode inside one MOSFET is installed on the upper edge of a copper strip (~18 cm), while the lower edge is immersed in LN_2 at 77 K. The above MOSFET assembly is installed at the terminal of moving shaft of a vertically-inverted stepper motor, as shown in Fig. 1. During the tests, the MOSFET is firstly heated up to about 350 °C by using a hot-air generator and then driven to get close to the liquid surface of the LN_2 along with the descending motion of the shaft. To monitor the real-time changing process of operating temperature T and its corresponding on-state resistance $R_{DS(on)}$, one Pt100 temperature sensor is directly stuck to the surface of drain electrode, and one 6 1/2 digital multimeter and one ±125-A hall-effect current sensor are used to collect the transient voltage and current data of the tested MOSFET for measuring the on-state resistance indirectly [9].

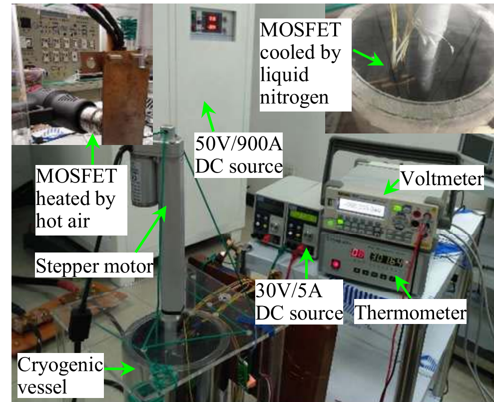

FIGURE 1. Photograph of the experimental testing set-ups.

III. RESULTS AND DISCUSSIONS

A. JUNCTION-TEMPERATURE-DEPENDENT $R_{DS(ON)}$ BEHAVIORS

To clarify the junction-temperature-dependent $R_{DS(on)}$ behaviors in the experiments, the testing drain current I_{DS} is set as a relatively low value of 0.2 A so that the measured temperature data collected by the Pt100 sensor is approximately equal to the real junction temperature. Fig. 2 shows the measured and fitted $R_{DS(on)}$ behaviors in these low-current tests. It can be seen that all the $R_{DS(on)}$ values in the five types of SiC MOSFETs decrease firstly and then increase as the operating temperature T decreases from about 350 K to 77 K. Due to the combined effects of electron mobility and ionized dopant concentration [18], the lowest on-state resistance R_{min} appears when both the maximum electron mobility and minimum carrier freeze-out effect are achieved. However, the corresponding optimal junction temperature T_{opt} might be varied with different microstructures and packages.

For instance, although Type A and C MOSFETs have almost the same R_{min} of ~73 mΩ, their corresponding T_{opt} in Table 1 are about 235 K and 275 K, respectively. Accordingly, practical junction temperature ranges should be within 201-276 K and 236-331 K when considering a suitable margin of $1.05 \times R_{min}$.

TABLE 1. Measured and fitted behaviors of the five types of SiC MOSFETs.

Type	R_{min} @T_{opt}	$R_{DS(on)} \leq 1.05\times R_{min}$	R_{min} @I_{DS}	$R_{DS(on)} \leq 1.05\times R_{min}$
A	73.9mΩ @235K	201-276K	80.2mΩ @24.3A	21.4-27.0A
B	169.3mΩ @370K	315-398K	203.9mΩ @14.7A	13.2-16.2A
C	73.2mΩ @275K	236-331K	79.3mΩ @24.6A	21.9-27.2A
D	24.4mΩ @180K	153-217K	23.9mΩ @34.8A	31.6-37.6A
E	70.2mΩ @300K	250-325K	89.0mΩ @23.0A	19.3-27.5A

To explain the experimental phenomena in Fig. 2, several works have reported the characterization of temperature dependences by considering the intrinsic mechanisms

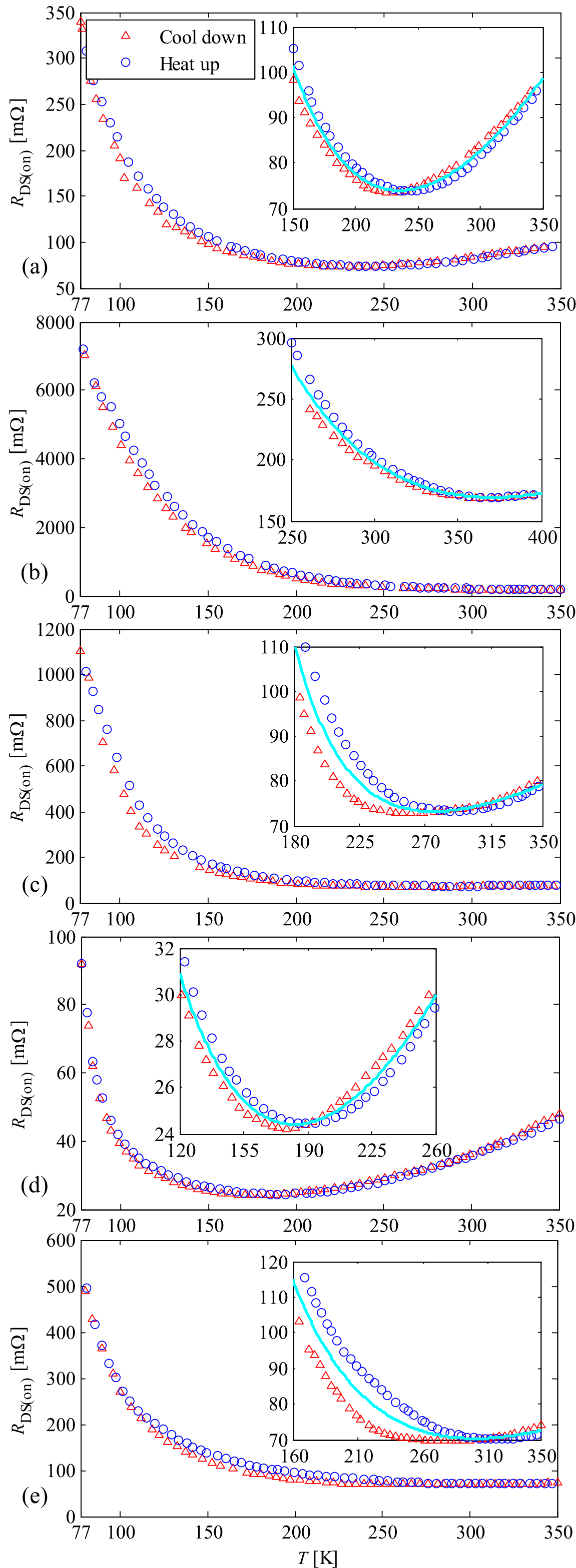

FIGURE 2. Measured and fitted $R_{DS(on)}$ behaviors in the five types of SiC MOSFETs from 350 K to 77 K: (a) $R_{DS(on)}$ in Type A; (b) $R_{DS(on)}$ in Type B; (c) $R_{DS(on)}$ in Type C; (d) $R_{DS(on)}$ in Type D; (e) $R_{DS(on)}$ in Type F.

of field-effect electronic devices [1]–[12]. However, these existing models are not easy to be used by power electronics engineers for designing practical cryogenic power

TABLE 2. Fitted parameters for the five types of SiC MOSFETs.

Type	p_1	p_2	p_3	p_4	p_5	p_6	p_7	p_8
A	626	-0.0154	19.74	0.00451	395.5	-0.085	0.917	0.143
B	6675	-0.0143	36.13	0.00356	1923	-0.196	3.656	0.222
C	4842	-0.0251	41.41	0.00182	437.6	-0.087	0.5407	0.160
D	152.4	-0.0180	6.897	0.00546	123	-0.054	0.0054	0.197
E	799.4	-0.0155	35.60	0.00189	659.6	-0.159	30.51	0.037

conversions. In view of engineering applications, a double-exponential function is introduced to visually represent the combined effects of electron mobility and ionized dopant concentration

$$\frac{R_{DS(on)}}{R_0} = p_1 \times \exp(p_2 \times \frac{T}{T_0}) + p_3 \times \exp(p_4 \times \frac{T}{T_0}) \quad (1)$$

where R_0 and T_0 are two normalized parameters of 1 Ω and 1 K, p_1 - p_4 are four fitted parameters that depend on the types of SiC MOSFET. Table 2 summarizes the fitted parameters in the five MOSFETs. From the fitted light blue lines in Fig. 2, these fitted functions match well with the measured $R_{DS(on)}$ values, and thus can be considered as the references for evaluating the junction-temperature-dependent $R_{DS(on)}$ behaviors. To further depict the relative changes of on-state resistance under different junction temperatures, one normalized factor R_{pu} is defined as the ratio of the $R_{DS(on)}$ at an arbitrary temperature to the $R_{DS(on)}$ at 300 K. Fig. 3 shows the normalized $R_{DS(on)}$ behaviors from 77 K to 350 K. These experimental results can be easily used to predict the optimal junction temperatures inside the five MOSFETs, and it is shown that all the lowest $R_{DS(on)}$ values appear at some higher temperatures over 77 K.

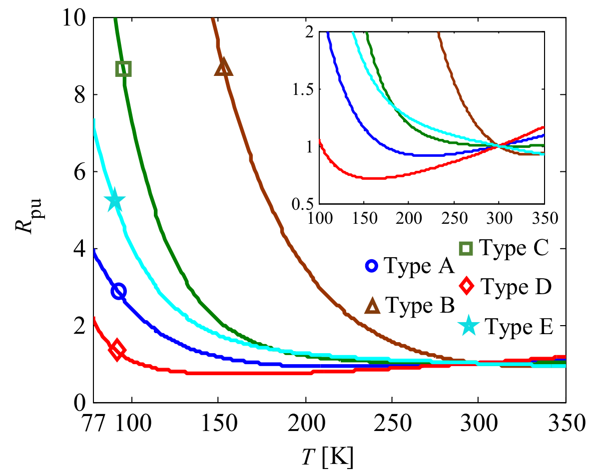

FIGURE 3. Normalized junction-temperature-dependent $R_{DS(on)}$ behaviors.

B. DRAIN-CURRENT-DEPENDENT $R_{DS(ON)}$ BEHAVIORS

Although all the optimal junction temperatures in Table 1 are higher than the LN_2 temperature at 77 K, SiC MOSFETs should be practically immersed in LN_2 for high-current operations in view of increasingly serious self-heating effects.

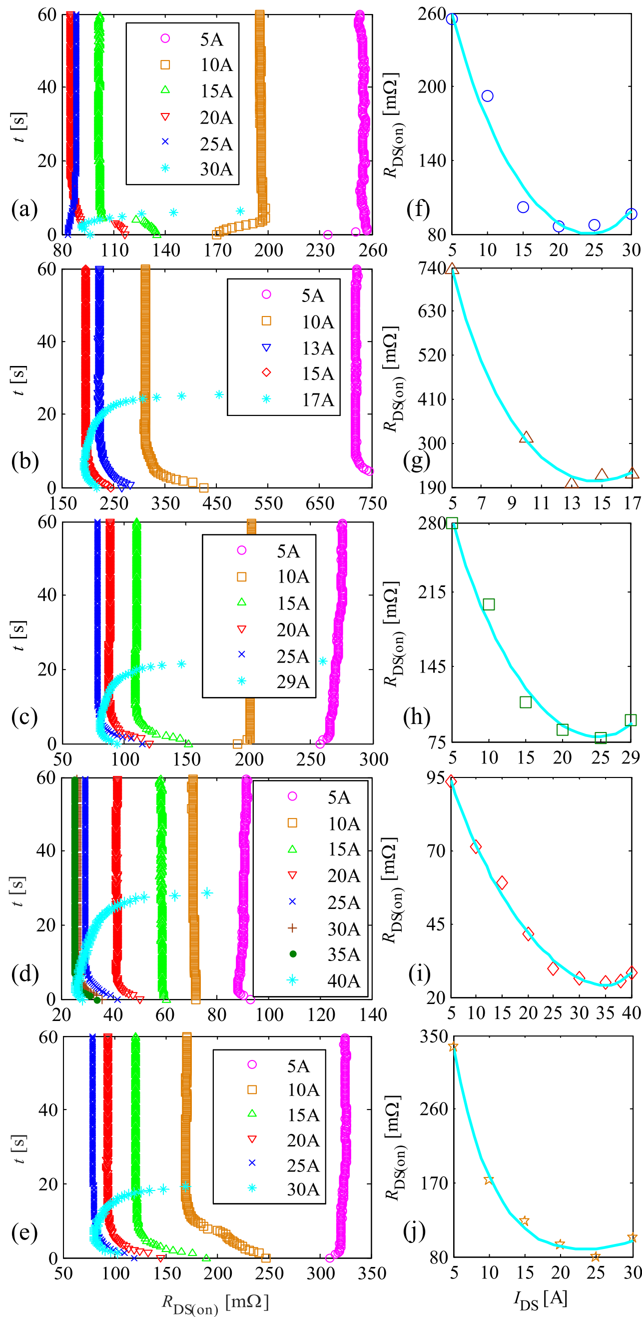

FIGURE 4. Transient and steady $R_{DS(on)}$ behaviors in the five types of SiC MOSFETs at 77 K: (a) Transient $R_{DS(on)}$ in Type A; (b) Transient $R_{DS(on)}$ in Type B; (c) Transient $R_{DS(on)}$ in Type C; (d) Transient $R_{DS(on)}$ in Type D; (e) Transient $R_{DS(on)}$ in Type F; (f) Steady $R_{DS(on)}$ in Type A; (g) Steady $R_{DS(on)}$ in Type B; (h) Steady $R_{DS(on)}$ in Type C; (i) Steady $R_{DS(on)}$ in Type D; (j) Steady $R_{DS(on)}$ in Type F.

Figs. 4(a)-(e) show the measured drain-current-dependent $R_{DS(on)}$ behaviors in one-minute high-current tests. It can be seen that most of the measured $R_{DS(on)}$ data are basically stabilized within about ten seconds along with the testing time t except for the turquoise data points obtained in those overcurrent tests. These stabilized $R_{DS(on)}$ values at t = 60 s are summarized in Figs. 4(f)-(j) in correspondence with the testing drain currents. Similar to the junction-temperature-dependent $R_{DS(on)}$ behaviors, all the $R_{DS(on)}$ values in Figs. 4(f)-(j) also decrease firstly and then increase as the I_{DS} increases from about 5 A to 40 A. This is mainly due to the dynamic power balance between transient power dissipation from the semiconductor materials and cooling power from the surrounding LN_2. Specifically, transient power dissipation increases quadratically with the drain current, and thus results in an obvious junction temperature rise inside the MOSFET. Meanwhile, thanks to the direct proportion between thermal conductivity and junction temperature [19], the increase of drain current also enhances the cooling power from the LN_2. Finally, the real junction temperature reaches a steady value when a dynamic power balance is achieved.

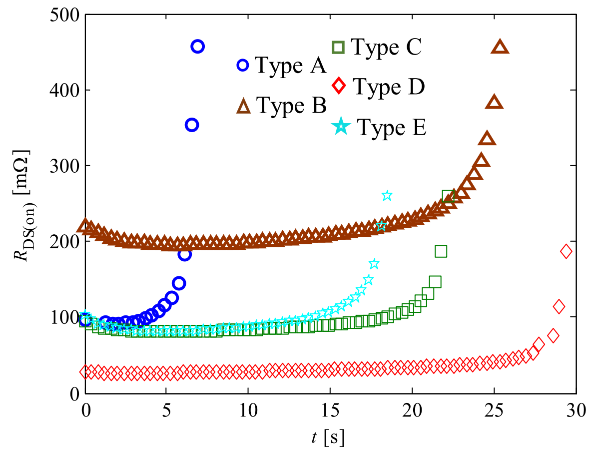

FIGURE 5. Transient $R_{DS(on)}$ behaviors under overcurrent conditions.

However, these dynamic power balances are unsustainable under some overcurrent operations. From the measured thermal runaway processes in Fig. 5, practical thermal-runaway time points are estimated to be ~6 s at 30 A, ~20 s at 17 A, ~20 s at 29 A, ~25 s at 40 A and ~15 s at 30 A for the five MOSFETs. These undesired phenomena are mainly due to the limited cooling power from the surrounding LN_2 to micro-sized packages of SiC MOSFETs. In other words, practical cooling power for the semiconductor materials inside one MOSFET is still limited even when the whole MOSFET is immersed in LN_2. Therefore, from the view of safe operation, practical drain current should be kept within its upper limit against the occurrence of thermal runaway.

In addition, from the view of efficient operation, practical drain current should be exactly rated at its optimal value when the lowest on-state resistance is reached. Fig. 6 shows the interactions among the on-state resistance, junction temperature and drain current for Type D MOSFET. The optimal operating range of drain current is about 31.6-37.6 A, while the corresponding junction temperature range is about 153-217 K accordingly. Assuming that a SiC-based cryogenic power conversion device has its operating current

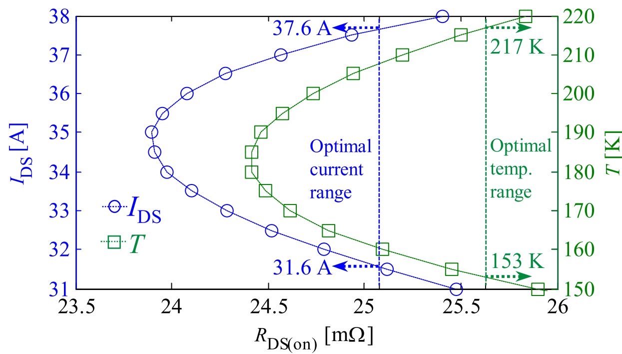

FIGURE 6. Interactions among the on-state resistance, junction temperature and drain current for Type D MOSFET.

rating of 350 A, ten Type D MOSFETs are then suggested to be connected in parallel. Considering the double-exponential functional relations in (1) and (2), too many or too few numbers will inevitably result in higher on-state resistances and higher power dissipations for the whole system.

Considering the interactions among the on-state resistance, junction temperature and drain current, the double-exponential function in (1) can also be used to depict the relation between the drain current and on-state resistance at 77 K

$$\frac{R_{DS(on)}}{R_0} = p_5 \times \exp(p_6 \times \frac{I_{DS}}{I_0}) + p_7 \times \exp(p_8 \times \frac{I_{DS}}{I_0}) \quad (2)$$

where $p_5 - p_8$ are four fitted parameters shown in Table 2.

These two junction-temperature-dependent and drain-current-dependent functions (1) and (2) visually depict the intrinsic interactions among the on-state resistance, junction temperature and drain current. This reveals that on-state resistance behaviors of commercial SiC MOSFETs at 77 K can be empirically characterized for the use in designing SiC-based cryogenic power conversion devices.

IV. CONCLUSION

In this paper, two junction-temperature-dependent and drain-current-dependent double-exponential functions have been extracted empirically from long-time experimental tests to characterize the cryogenic on-state resistance behaviors of commercial SiC MOSFETs. These two simple mathematical functions visually depict the intrinsic interactions among the on-state resistance, junction temperature and drain current, and thus lay some empirical bases for designing practical SiC-based cryogenic power conversion systems.

REFERENCES

[1] S. Z. Chen, C. F. Cai, T. Wang, Q. Guo, and K. Sheng, "Cryogenic and high temperature performance of 4H-SiC power MOSFETs," in *Proc. 28th Annu. IEEE Appl. Power Electron. Conf. Expo.*, Mar. 2013, pp. 207–210.

[2] L. J. Woodend *et al.*, "Cryogenic characterisation and modelling of commercial SiC MOSFETs," in *Proc. Eur. Conf. Silicon Carbide Related Mater.*, Sep. 2016, pp. 557–560.

[3] K. Tian *et al.*, "Characterization of 1.2 kV 4H-SiC power MOSFETs and Si IGBTs at cryogenic and high temperatures," in *Proc. 14th China Int. Forum Solid-State Light. Int. Forum Wide Bandgap Semicond. China*, Nov. 2017, pp. 140–143.

[4] B. J. Baliga, *Fundamentals of Power Semiconductor Devices*. New York, NY, USA: Springer, 2008, pp. 358–365.

[5] Z. Chen, Y. Y. Yao, D. Boroyevich, K. D. T. Ngo, P. Mattavelli, and K. Rajashekara, "A 1200-V, 60-A SiC MOSFET multichip phase-leg module for high-temperature, high-frequency applications," *IEEE Trans. Power Electron.*, vol. 29, no. 5, pp. 2307–2320, May 2014.

[6] S. Chowdhury, C. W. Hitchcock, and T. P. Chow, "Comparative evaluation of commercial 1200 V SiC power MOSFETs using diagnostic I-V characterization at cryogenic temperatures," in *Proc. Eur. Conf. Silicon Carbide Related Mater.*, Sep. 2016, pp. 545–548.

[7] K. Yano, Y. Tanaka, and M. Yamamoto, "Extremely low ON-resistance SiC cascode configuration using buried-gate static induction transistor," *IEEE Electron Device Lett.*, vol. 39, no. 12, pp. 1892–1895, Dec. 2018.

[8] M. Riccio, V. D'Alessandro, G. Romano, L. Maresca, G. Breglio, and A. Irace, "A temperature-dependent SPICE model of SiC power MOSFETs for within and out-of-SOA simulations," *IEEE Trans. Power Electron.*, vol. 33, no. 9, pp. 8020–8029, Sep. 2018.

[9] H. Li, X. L. Liao, Y. G. Hu, Z. Zeng, E. B. Song, and H. W. Xiao, "Analysis of SiC MOSFET dI/dt and its temperature dependence," *IET Power Electron.*, vol. 11, no. 3, pp. 491–500, Mar. 2018.

[10] W.-C. Lien, N. Damrongplasit, J. H. Paredes, D. G. Senesky, T.-J. K. Liu, and A. P. Pisano, "4H-SiC N-channel JFET for operation in high-temperature environments," *IEEE J. Electron Devices Soc.*, vol. 2, no. 6, pp. 164–167, Nov. 2014.

[11] H. D. Gui *et al.*, "Characterization of 1.2 kV SiC power MOSFETs at cryogenic temperatures," in *Proc. 10th IEEE Energy Convers. Congr. Expo.*, Sep. 2018, pp. 7010–7015.

[12] Z. Y. Zhang *et al.*, "Characterization of wide bandgap semiconductor devices for cryogenically-cooled power electronics in aircraft applications," in *Proc. AIAA/IEEE Elect. Aircraft Technol. Symp.*, Jul. 2018, pp. 1–8.

[13] F. J. De la Hidalga, M. J. Deen, and E. A. Gutierrez, "Theoretical and experimental characterization of self-heating in silicon integrated devices operating at low temperatures," *IEEE Trans. Electron Devices*, vol. 47, no. 5, pp. 1098–1106, May 2000.

[14] T. T. Mnatsakanov, M. E. Levinshtein, L. I. Pomortseva, and S. N. Yurkov, "Carrier mobility model for simulation of SiC-based electronic devices," *Semicond. Sci. Technol.*, vol. 17, no. 9, pp. 974–977, Aug. 2002.

[15] Y. Chen *et al.*, "Experimental investigations of state-of-the-art 650-V class power MOSFETs for cryogenic power conversion at 77K," *IEEE J. Electron Devices Soc.*, vol. 6, no. 1, pp. 8–18, Jan. 2018.

[16] X. Y. Chen *et al.*, "An efficient boost chopper integrated with cryogenic MOSFETs and HTS inductor," *IEEE Trans. Appl. Supercond.*, vol. 26, no. 7, Oct. 2016, Art. no. 5701606.

[17] J. X. Jin, X. Y. Chen, L. Wen, S. C. Wang, and Y. Xin, "Cryogenic power conversion for SMES application in a liquid hydrogen powered fuel cell electric vehicle," *IEEE Trans. Appl. Supercond.*, vol. 25, no. 1, Feb. 2015, Art. no. 5700111.

[18] S. Potbhare, N. Goldsman, A. Lelis, J. M. McGarrity, F. B. McLean, and D. Habersat, "A physical model of high temperature 4H-SiC MOSFET," *IEEE Trans. Electron Devices*, vol. 55, no. 8, pp. 2029–2040, Aug. 2008.

[19] D. P. Foty and S. L. Titcomb, "Thermal effects in n-channel enhancement MOSFET's operated at cryogenic temperatures," *IEEE Trans. Electron Devices*, vol. 34, no. 1, pp. 107–113, Jan. 1987.

KANG HONG is currently pursuing the B.S. degree in electrical engineering with Sichuan Normal University, Chengdu, China.

XIAO-YUAN CHEN received the B.S. degree from the Chengdu University of Technology, Chengdu, China, in 2007, and the Ph.D. degree from the University of Electronic Science and Technology of China, Chengdu, in 2015. He is currently an Associate Professor with the School of Engineering, Sichuan Normal University, Chengdu. His research interests include cryogenic power electronics, low-voltage direct-current superconducting power transmission and distribution, and hybrid electrical-chemical energy transfer and utilization.

YU CHEN received the B.S. degree from Sichuan Normal University, Chengdu, China, in 2018, where she is currently pursuing the M.S. degree in safety engineering.

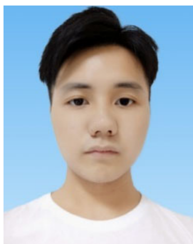

MING-SHUN ZHANG is currently pursuing the B.S. degree in electrical engineering with Sichuan Normal University, Chengdu, China.

JIA-LEI WANG is currently pursuing the B.S. degree in electrical engineering with Sichuan Normal University, Chengdu, China.

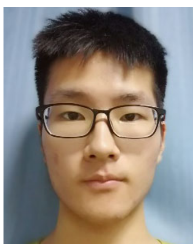

SHAN JIANG is currently pursuing the B.S. degree in electrical engineering with Sichuan Normal University, Chengdu, China.

ZHOU PANG is currently pursuing the B.S. degree in electrical engineering with Sichuan Normal University, Chengdu, China.

HAN-MEI YANG is currently pursuing the B.S. degree in electrical engineering with Sichuan Normal University, Chengdu, China.

NING XUE is currently pursuing the B.S. degree in electrical engineering with Sichuan Normal University, Chengdu, China.

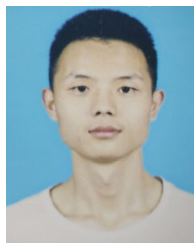

HUA-YU GOU is currently pursuing the B.S. degree in electrical engineering with Sichuan Normal University, Chengdu, China.

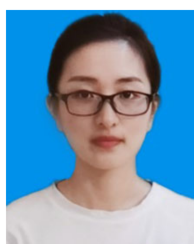

LEI ZENG received the B.S. degree from Sichuan Normal University, Chengdu, China, in 2017, where she is currently pursuing the M.S. degree in safety engineering.